Biomaterials 33 (2012) 668–678

Contents lists available at SciVerse ScienceDirect

Biomaterials

journal homepage: www.elsevier.com/locate/biomaterials

Hydrogel swelling as a trigger to release biodegradable polymer microneedles in skin

MinYoung Kim [a,1], Bokyung Jung [b,1], Jung-Hwan Park [a,*]

[a] College of BioNano Technology and Gachon BioNano Research Institute, Gachon University, Seongnam-si, Gyeonggi-do 461-701, Republic of Korea
[b] Department of Chemical and Biomolecular Engineering, KAIST, Guseongdong, Yuseong-gu, Daejeon 305-701, Republic of Korea

ARTICLE INFO

Article history:
Received 7 September 2011
Accepted 27 September 2011
Available online 13 October 2011

Keywords:
Biodegradable polymer
Microneedle
Swelling of hydrogel
Transdermal drug delivery

ABSTRACT

Biodegradable polymeric microneedles were developed as a method for achieving sustained transdermal drug release. These microneedles have potential as a patient-friendly substitute for conventional sustained release methods. However, they have limitations related to the difficulty of achieving separation of the needles into the skin. We demonstrated that microneedle separation into the skin was mediated by hydrogel swelling in response to contact with body fluid after the needles were inserted into the skin. The hydrogel microparticles were synthesized by an emulsification method using poly-N-isopropylacrylamide (PNIPAAm). The microneedles were fabricated by micromolding poly-lactic-co-glycolic acid (PLGA) after filling the cavities of the mold with the hydrogel microparticles. The failure of microneedle tips caused by hydrogel swelling was studied in regard to contact with water, insertion of microneedles into porcine cadaver skin *in vitro*, stress–strain behavior, and insertion into the back skin of a hairless mouse *in vivo*. The drug delivery property of the hydrogel particles was investigated qualitatively by inserting polymer microneedles into porcine cadaver skin *in vitro*, and the sustained release property of PLGA microneedles containing hydrogel microparticles was studied quantitatively using the Franz cell model. The hydrogel particles absorbed water quickly, resulting in the cracking of the microneedles due to the difference in volume expansion between the needle matrix polymer and the hydrogel particles. The swollen particles caused the microneedles to totally breakdown, leaving the microneedle tips in the porcine cadaver skin *in vitro* and in the hairless mouse skin *in vivo*. Model drugs encapsulated in biodegradable polymer microneedles and hydrogel microparticles were successfully delivered by releasing microneedles into the skin.

1. Introduction

Various kinds of drugs must be delivered continuously over a predetermined period to maintain a therapeutic dose and to reduce side effects caused by too rapid delivery [1]. The most frequently used drug delivery systems, which can release drugs over a prolonged period of several days, involve parenteral injection of biodegradable microspheres, liposomes, and emulsions [2,3]. Sustained drug delivery using a transdermal patch has been developed to provide controlled, non-invasive release of medication. Transdermal drug delivery avoids the pain and inconvenience of injection [4]. However, the transdermal delivery system has limits because of the low permeability of drugs into the skin and the molecular weight limit of drugs for transport through the stratum corneum [5]. The microneedle system has been developed to overcome these limitations.

Previous studies with microneedles have demonstrated that skin permeability can be increased by orders of magnitude for delivery of peptide, protein, vaccines and nanoparticles [6–10]. Various types of microneedles have been developed for active transdermal drug delivery and are classified as solid, drug-coated [11], and drug-loaded [12,13], depending on the method of drug application. (1) Solid microneedles have been used to pierce the skin, increasing the permeability of drugs through the stratum corneum [14]. However, the delivery rate of drugs through holes generated by solid microneedles is diminished by the quick closing of the holes, and there is a chance of cross-contamination by a sharps hazard [15]. (2) Drug-coated microneedles are prepared by applying a specially formulated drug solution to in-plane microneedles using a dip-coating process [16–18]. These microneedles have advantages of easy application and rapid delivery. However, there is biohazardous waste of sharp microneedles and sustained delivery is difficult due to the rapid dissolution of the coating

* Corresponding author. Tel.: +82 31 750 8551; fax: +82 31 750 8757.
E-mail address: pa90201@kyungwon.ac.kr (J.-H. Park).
[1] These authors equally contributed to this work.

0142-9612/$ – see front matter © 2011 Elsevier Ltd. All rights reserved.
doi:10.1016/j.biomaterials.2011.09.074

material. (3) Drug-loaded microneedles are made of water-dissolving cellulose, maltose, and dextrin [6,12,19–23]. These microneedles do not leave sharp tips after use and provide effective drug delivery by leaving microneedle material in the skin as a drug depot. However, upon contact with water in the skin, they hydrate and quickly form a weak gel, resulting in too rapid drug delivery, and it is difficult to sustain drug delivery because the needle material dissolves quickly [12].

Previous work has demonstrated that a biodegradable polymer can be utilized for controlled drug delivery by encapsulating a model drug inside microneedles, which can release the model drug over a predetermined period according to the formulations. A previous study showed the possibility of these biodegradable microneedles as a patient-friendly substitute for conventional sustained delivery methods [24]. However, these microneedles must be inserted and remain in the skin for several days to effectively utilize the degradation property of biodegradable polymer. The use of biodegradable polymer microneedles is therefore subject to the limitation of a long period of insertion [24]. Thus, to achieve patient-friendly use, it is necessary to develop a feasible microneedle system using biodegradable polymer to replace conventional sustained release methods of transdermal drug delivery.

Hydrogel is defined as a polymeric network of microparticles that swell to several times their original volume while remaining insoluble in aqueous solutions [25,26]. Hydrogel differs from hydrophobic polymers such as poly-lactic acid (PLA) and poly-lactic-co-glycolic acid (PLGA), which have limited water absorption capabilities (below 5%) [27]. Because the favorable properties of hydrogel are its hydrophilicity and biocompatibility, hydrogel has been studied as a drug delivery carrier [28,29]. Hydrogel response has been designed by a gelling mechanism determined by pH, ionic strength, and temperature [30–32]. Materials selection and network fabrication govern the rate and mode of drug release from hydrogel matrices [33–37].

In this paper, we describe the design of PLGA microneedles encapsulating hydrogel microparticles. This design is intended as an effective way to deliver both hydrophilic and hydrophobic drugs in a sustained manner by facilitating the failure of the microneedles as a result of the swelling of hydrogel particles after the microneedles have been inserted into the skin. Hydrogel particles expand quickly by absorbing water, which triggers cracks and partial mechanical failure of the microneedles due to the difference in volume expansion between the needle matrix polymer and the particles. Then, highly swollen hydrogel microparticles cause mechanical failure of microneedles quickly due to mechanical weakness of swollen gel. In addition to causing the failure of the inserted microneedles, the hydrogel particles serve as a carrier of hydrophilic drugs. The capability of carrying hydrophilic and hydrophobic drugs can be achieved by using hydrogel particles and biodegradable polymers simultaneously. In this paper, we report the measurement of (1) the physicochemical properties of hydrogel particles and (2) the response of the microparticles to water absorption as a function of time. The mechanical failure of PLGA microneedles as a result of the swelling of hydrogel particles was observed by optical investigation as function of contact time with water and the content of hydrogel microparticles in microneedles. The drug delivery properties of the dual delivery system were observed to demonstrate the potential of the new system by using *in vitro* and *in vivo* experiments.

2. Materials and methods

2.1. Preparation and characterization of hydrogel particles

Hydrogel synthesis was conducted by free radical cross-linking copolymerization at room temperature in a nitrogen atmosphere. Using sonication for 10 min, 26.5 mmol of N-isopropylacrylamide (NIPAAm, Sigma–Aldrich, St. Louis, MO), 0.778 mmol of N,N′-methylenebisacrylamide (MBAAm, Sigma–Aldrich), and 1.31 mmol of ammonium persulfate (Sigma–Aldrich) were dissolved in deionized water. Nitrogen bubbling for 30 min was used to mix 8.75 mmol of SPAN 80 and 150 ml of n-hexane (J.T. Baker, Phillipsburg, NJ). Then 30 ml of the aqueous solution with monomers, a cross-linking agent, and an initiator were added to 150 ml of the hexane with SPAN 80 (Sigma–Aldrich) for 30 min under nitrogen gas. Three milliliters of tetramethylethylenediamine (TEMED, Sigma–Aldrich) with 20.1 mM of concentration was slowly added dropwise into the mixture. This reaction was maintained for 4 h. The cross-linked microparticles were intensively washed with a mixture of acetone (Daejung Chemicals & Metals Co., Ltd., Shiheung, South Korea) and deionized water (1:1 vol%) to remove surfactant. In addition, the reaction mixture was washed with deionized water for 3 days, and finally hydrogel microparticles were obtained by freeze-drying (Freeze dryer DC400, Yamato Scientific Co., Ltd., Tokyo, Japan).

A glass slide was placed on a silicone rubber heater (Silicone Rubber Heater, Nissi-Ygc Co., Ltd., Anyang, South Korea) and a K type thermocouple (Flexible view probe, Cole Parmer, Chicago, IL) was attached to the slide. The response of hydrogel particles was investigated at 32 °C. The silicon rubber heater was controlled by using a thermo-controller (Digi-Sense, Vernon Hills, IL) for maintaining the predetermined temperature of the sample. Dry hydrogel particles were spread on the slide (Microscope Slide 7101, Woody International Trading Co., Ltd., Yancheng, China) and then the slide was put on a fluorescence microscope (Eclipse TE2000-U, Nikon, Tokyo, Japan) with a video recording program. 100 μl of phosphate buffered saline (PBS) was dropped onto the hydrogel particles and the volume change of the particles as a result of water absorption was observed using the microscope at 100× magnification. Streaming video from the microscope recorded the volume change for a predetermined period (Camtasia, TechSmith, Okemos, MI). After recording was completed, the images were captured every 0.5 s for 1 min and the diameter of particles at each time point was measured. Then the increase in average volume of the particles was calculated.

2.2. Fabrication of microneedles with hydrogel particles

Microneedles with hydrogel particles were prepared by micromolding PLGA 50/50 (inherent viscosity 0.58 dL/g, Sur Modics Pharmaceuticals Inc., Birmingham, AL) in a poly-di-methyl siloxane (PDMS, Sylgard 184, Dow Corning, MI) microneedle mold. Six kinds of microneedles were prepared by filling hydrogel particles in cavities 1, 2, 3, 4, 5, and 6 times, respectively. The hydrogel particles were spread on the mold cavities and then pushed into the cavities using the master microneedle structure. The same filling procedure was repeated sequentially up to the predetermined filling number. Residual particles on the surface of the mold were removed using adhesive tape (3 M Company, St. Paul, MN). The mold was then filled with melted PLGA and placed in a vacuum oven at 150 °C under 100 kPa of pressure for 30 min. The resulting microneedles containing hydrogel particles were manually removed from the mold after being cooled (Fig. 1). Salt particles (sodium chloride, Sigma–Aldrich) were pulverized and then filtered with sieves (ChungGye Industrial Mfg., Seoul, South Korea) to obtain particles between 10 and 50 μm in size. PLGA microneedles with salt particles and solid PLGA microneedles without hydrogel particles were fabricated in the same way.

2.3. Insertion test of microneedles with hydrogel particles

To examine the successful insertion into the skin of hydrogel-containing microneedles regarding hydrogel particle content in microneedles, three arrays of 100 microneedles with 18% (v/v), 31% (v/v), 53% (v/v), and 68% (v/v) hydrogel microparticle content, respectively, were pushed into the full thickness of human cadaver skin with a strength of 20 N for 5 s using a compression force station (HAP-0015, Hana Technology, Seoul, South Korea). Then the pierced skin was stained with Trypan Blue (Sigma–Aldrich) for 5 min. Excess dye was removed and the skin was evaluated for the appearance of blue dots on the stratum corneum using an optical microscope (sv-35, Sometech, Seoul, South Korea). The number of stained holes was counted in each of the three arrays.

2.4. Characterization of microneedle failure by hydrogel swelling

The effect of volume expansion on microneedle failure caused by hydrogel swelling was observed during contact with water without applying external force to the microneedles. Microneedle failure caused by both mechanical weakness and volume expansion of hydrogel was studied by measuring stress–strain behavior after water contact and by inserting and removing microneedles into hydrated skin layers *in vitro* and *in vivo*.

To verify the effect of volume expansion of hydrogel particles on microneedle failure, we investigated the gradual failure of microneedles by contact with PBS solution at 32 °C. Microneedles containing hydrogel particles were placed on a glass slide at 32 °C constant temperature, and 100 μl of PBS at 32 °C was dropped on microneedles containing 53% (v/v) of hydrogel particles. Then residual PBS on the surface was removed at 0, 10, 30 and 60 s and quickly vacuum dried. The geometrical

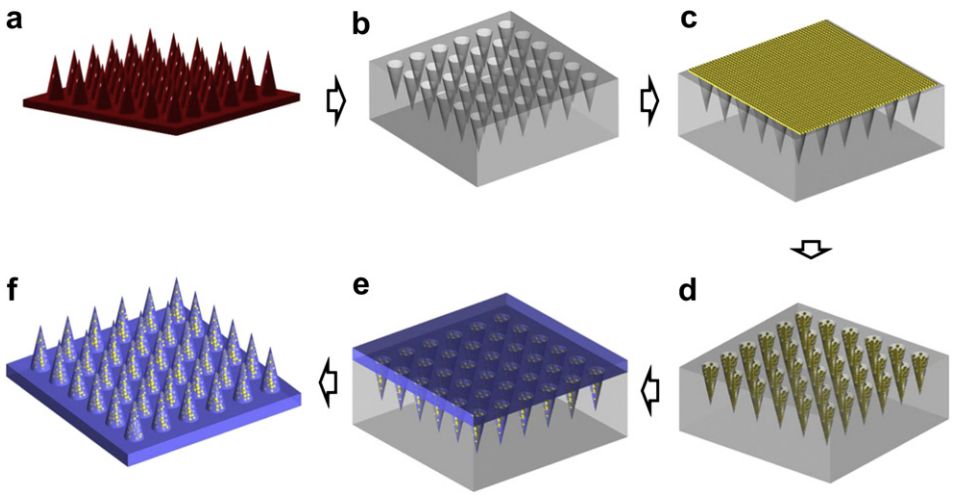

Fig. 1. Diagram of fabrication process of hydrogel integrated biodegradable polymer microneedle (a) preparation of PDMS female mold out of PDMS male master, (b) PDMS female mold, (c) cover of hydrogel particles (d) filling hydrogel particles in the cavities of micromold using master structure (e) PLGA on the PDMS mold and molding PLGA in vacuum oven, and (f) thermally molded PLGA microneedles integrating hydrogel particles.

changes in the dried microneedles were compared by taking images using a scanning electron microscope (SEM, JSM-7001F, JEOL Ltd., Tokyo, Japan).

The gradual failure of microneedles containing 31% (v/v) of hydrogel microparticles after insertion into the full thickness of porcine cadaver skin *in vitro* was investigated optically. Microneedles were compressed into porcine cadaver skin for predetermined times of 1 min, 5 min, 15 min, and 30 min with 20 N of force generated by a compression mold press (HAP-0015, Hana Technology) at 32 °C. The same investigation process by SEM was repeated for the samples that had come into contact with PBS. The length of remaining microneedles was measured from SEM images, and the change in length was investigated in terms of insertion time.

To compare the stress–strain behavior of PLGA microneedles regarding hydrogel content, 100 μl of PBS at 32 °C was dropped on three arrays of microneedles containing 0% (v/v), 18% (v/v), and 31% (v/v), respectively, of hydrogel particles for 5 min. PLGA microneedles with 31% (v/v) hydrogel microparticle content were placed in contact with PBS for 0 min, 5 min, and 15 min, respectively, to observe the effect of water exposure time on the mechanical behavior of the microneedles. Residual PBS was then removed. To determine the stress–strain behavior of the microneedles, a displacement-force test station (Model 921A, Tricor System, Elgin, IL) was used. Stress–strain curves were generated by measuring force and displacement while the test station pressed an array of microneedles against a metal surface at a rate of 1.1 mm/s. The applied force was divided by the number of microneedles and then the force applied to a microneedle, and its displacement was calculated.

Microneedles with 31% (v/v) hydrogel particle content were inserted into the back skin of a hairless mouse (20–25 g, Orient Bio., Seongnam, South Korea) and were fixed by bandage (Derma Plast, IVF Hartmann, Neuhausen, Switzerland) for 60 min. For comparison, solid PLGA microneedles and PLGA microneedles encapsulating salt particles with a similar range in size and a similar volume of hydrogel particles were also inserted into the back skin of a hairless mouse for 60 min. Using SEM, the morphological change in microneedles containing hydrogel particles was compared with changes in solid PLGA microneedles and PLGA microneedles containing salt microparticles. All animal care and experimental procedures were approved by the Animal Care and Use Committee of Kyungwon University.

2.5. Storage stability of microneedles at high humidity condition

To examine the stability of microneedles containing hydrogel microparticles against high humidity, microneedles with hydrogel microparticles were stored in a high humidity condition and their water stability was compared with that of water-dissolving microneedles made of sodium carboxymethyl cellulose (CMC; Sigma–Aldrich). Microneedles containing 31% (v/v) of hydrogel microparticles and CMC microneedles were stored in the incubator (Sanyo MIR-162, Sanyo Electric Co., Ltd., Osaka, Japan) at 95% humidity. Samples were taken out of an incubator at 1, 5, and 12 h and dried in a desiccator. Then the morphological change of individual microneedles in an array was investigated by SEM.

2.6. Drug delivery property of dual system

Calcein (Sigma–Aldrich) was used as a hydrophilic model drug delivered by using hydrogel microparticles. Microparticles were dispersed in a 1 mM calcein solution for 30 min, then trapped on a membrane filter with 0.8 μm pore size (cellulose acetate filter, Advantec MFS, Inc., Pleasanton, CA), and subsequently washed with anhydrous ethanol (J.T. Baker) to remove calcein solution remaining on the surface. Finally, particles with calcein were dried under vacuum at room temperature.

An array of microneedles was inserted into the full thickness of porcine cadaver skin at 32 °C *in vitro* for 15 min and removed. The diffusion of calcein in the porcine cadaver skin was observed at 0 min, 15 min, and 60 min after removal of the microneedles, and the intensity and distribution of calcein was measured using identical exposure conditions by a fluorescence microscope (Eclipse 80i, Nikon). The fluorescence image of the skin was repainted to get a clear vision through color-mapping by using a homemade code for better understanding of the relative difference in intensity. First, pixel information about the green color was extracted by filtering out red and blue colors to eliminate unnecessary light information from the fluorescence image. Then the intensity information of the green color images was repainted to show the gradual change in color from blue (0 intensity) to red (max intensity).

Rhodamine salt particles (101 inner salt, Sigma–Aldrich), 1–3 μm in diameter, were mixed with PLGA melted on a 200 °C hot plate, and the mixture was cooled down to be a solid at room temperature. Hydrogel microparticles filled the cavities of the mold. The solid PLGA with rhodamine particles was placed on the mold, and PLGA microneedles encapsulating hydrogel microparticles and rhodamine salt were copied from the mold in an oven set at 150 °C under vacuum. The release pattern of PLGA microparticles with hydrogel and rhodamine was compared with that of water-soluble microneedles to demonstrate the sustained release property of the PLGA microneedle system. Two different microneedle arrays were inserted through 100-μm thick sealing film (parafilm, Curwood Inc., Oshkosh, WI) and then sealed with parafilm so that only the needle tips were exposed. Then the microneedle tips were pressed into a human cadaver epidermis layer about 250 μm thick (Hans Biomed., Seoul, Korea) with 20 N of force. The human cadaver epidermis containing microneedles was mounted on a Franz cell, and the microneedles were removed from the epidermis after 1 h. The receptor chamber was filled with PBS as soon as the epidermis with microneedles was placed between the chambers of the Franz cell. Then 100 μl of solution was sampled and the same volume of PBS was placed in the receptor chamber at predetermined times of 20 min, 2 h, 6 h, 24 h, 48 h, 72 h, 120 h, and 144 h. The fluorescent intensity of the sample solution was measured using a fluorescence spectrophotometer (Cary Eclipse, Varaian Inc. Palo Alto, CA). The concentration was calculated using a calibration curve.

To investigate the remaining hydrogel particles and PLGA needles in the skin and the skin covering the tips of the microneedles after microneedle separation because of hydrogel swelling, fluorescein-5-isothiocyanate (FITC)–labeled hydrogel particles were utilized. FITC was conjugated to hydrogel copolymerized with acrylic acid (AA, Sigma–Aldrich) within the molar ratio of AA to NIPAAm. First, AA (0.26 mmol, 1 mol % to NIPAAm) was copolymerized with NIPAAm and cross-linked with the same synthetic scheme. Free amine was introduced to a carboxylic group of AA by using EDC and NHS protocol. Then FITC was conjugated to free amine by forming a thiourea linkage. FITC-labeled particles were encapsulated in PLGA microneedles by the molding method described earlier. Microneedles were inserted into the back skin of a hairless mouse and were fixed by bandage (Derma Plast, IVF Hartmann, Neuhausen, Switzerland) for 30 min. Then the part of the skin treated with microneedles was investigated at 1 h, 1 day, and 3 days using a fluorescence microscope (SMZ1500, Nikon). The tips of microneedles containing hydrogel microparticles left in the mouse skin layer were observed *in vivo*.

The skin sample was placed vertically in a freezing block filled with an optimal cutting temperature solution (Tissue-Tek O.C.T., Sakura® Finetechnical Co., Ltd., Tokyo, Japan). Then the sample was frozen to −72 °C before being taken for cryostat cutting. The frozen sample was sectioned using a cryostat microtome (HM 560, Microm, Walldorf, Germany) and investigated to define the status of PLGA microneedles and hydrogel particles in mouse skin using a fluorescence microscope (Eclipse 80i, Nikon).

3. Results and discussion

3.1. Polymer microneedles with hydrogel microparticles

3.1.1. Characterization of hydrogel particles

The physicochemical properties of prepared hydrogel particles were investigated by measuring their volume expansion quantitatively. First, we compared the size of the air-dried powder form of hydrogel particles and pre-swollen hydrogel particles in PBS, which were imaged by SEM and optical microscopy (OM; TE-2000, Nikon), respectively (Fig. 2). The hydrogel microparticles had a spherical shape as a result of the emulsification method. The size of dry microparticles was controlled by a surfactant and agitation condition that kept them around 30 μm in diameter, an optimum size that facilitates filling the cavities of the mold with the microparticles. The dried hydrogel particles averaged 30 ± 10 μm in diameter, while those swelled by PBS averaged 70 ± 15 μm in diameter. As confirmed by SEM and OM measurements, volume expansion of hydrogel microparticles encapsulated in PLGA microneedles significantly influences mechanical failure of microneedles when they are in contact with body fluid under the skin. PNIPAAm was selected as the hydrogel material because its swelling behavior and mechanical properties are well defined. We needed hydrogel with fast volume expansion and rapid loss of mechanical strength as a result of water absorption. Also, a microspherical shape 10–40 μm in diameter was needed to encapsulate them in microneedles with a base diameter of 250 μm using the micromolding method and to maximize the effectiveness of hydrogel swelling on needle failure. PNIPAAm hydrogel has a fast water absorption rate and a high swelling ratio. Also, PNIPAAm hydrogel microspheres could be obtained with the emulsification method used in this study. Young's moduli of a highly swollen state of PNIPAAm gel at 30 °C is 200 times lower than for a dry state at room temperature, and such a drastic loss of mechanical strength was appropriate for causing mechanical failure of microneedles. In this study, PNIPAAm hydrogel particles not only triggered the mechanical fracture of PLGA microneedles by well-controlled volumetric expansion and rapid loss of mechanical strength, but they also played a role as a depot for delivery of hydrophilic drugs. PNIPAAm hydrogel is controversial from the point of view of human safety of the new microneedle system because the microneedles with hydrogel microparticles remain in the skin for some time. Thus the toxicity and biodegradability of PNIPAAm hydrogel should be considered. PNIPAAm hydrogel was reported to have no toxicity toward dermal fibroblasts [38], and few hydrogel systems have been developed recently that are clinically safe to remain in the skin for 24 months [39]. Non-degradable PNIPAAm hydrogel was used in this study primarily because it was easier to control its swelling behavior. PNIPAAm hydrogel can be made biodegradable by using biodegradable oligopeptide crosslinker instead of MBAAm [40]. However, PNIPAAm segment is not usually biodegradable and therefore a PNIPAAm hydrogel system should be carefully designed to allow clearance of the hydrogel from the body after PNIPAAm hydrogel is degraded into PNIPAAm segments [41]. Non-biodegradable polymer segments from hydrogel are cleared mainly

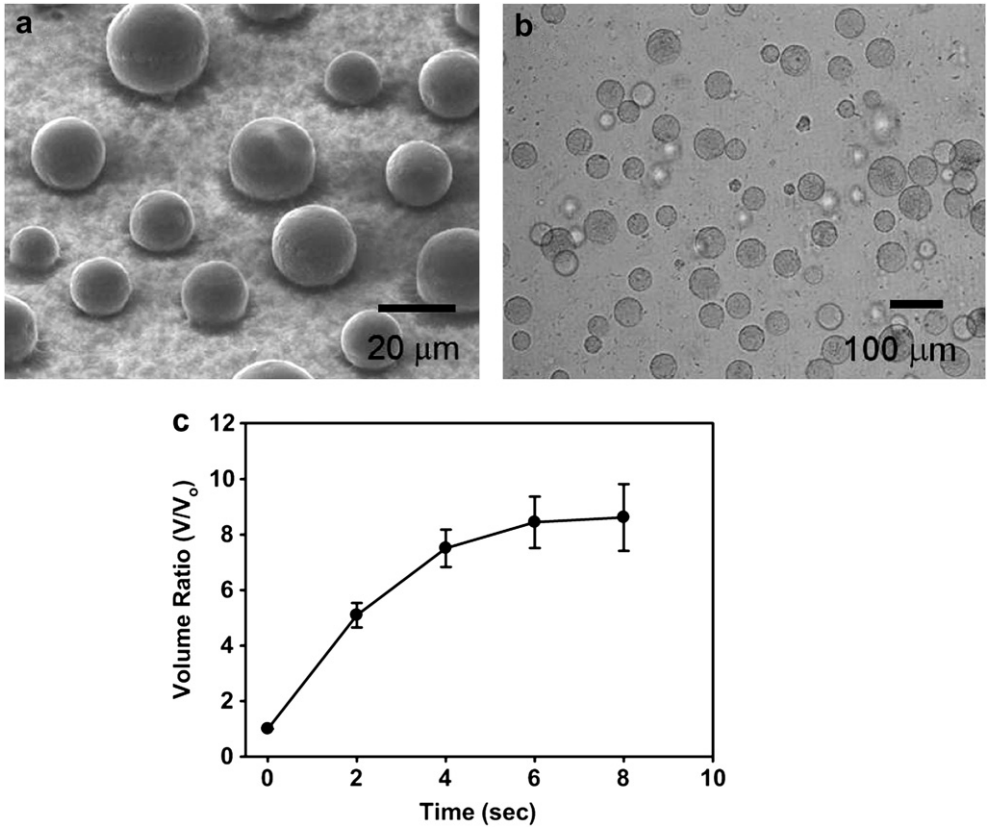

Fig. 2. (a) Scanning electron microscope image of air-dried hydrogel particles and (b) optical image of swollen hydrogel particles in PBS at 32 °C. Histogram showing the size distribution of (c) change in volume of swollen hydrogel particles compared to the volume of dried particles at 32 °C regarding time.

by renal excretion, which is controlled primarily by the hydrodynamic volume of the polymer chains. PNIPAAm segments with molecular weight below 40 kDa can be cleared from the body by renal excretion [42,43]. Thus PNIPAAm gel can be excreted by the renal filtration process by degrading segments below 40 K molecular weight using an appropriate cross-linking method. For practical application, a biodegradable hydrogel system will be utilized in our next experiment. In this study, the feasibility of responsive failure of microneedles was examined by using hydrogel microparticles for separation of microneedle in skin. The volumetric expansion of PNIPAAm hydrogel microparticles levels off after 6 s as the microneedles make contact with PBS, maintaining approximately eight times the volume of the original particles. The standard deviation and average size of hydrogel particles were determined by image analyzer of captured image of particles by microscope at predetermined conditions. The eight-fold volume expansion at 6 s after contact with PBS is sufficient to cause the mechanical breakdown of microneedles. In addition to volume expansion, the mechanical failure of microneedles was caused by a drastic reduction of mechanical strength because dried PNIPAAm hydrogel has 914 kPa of Young's moduli and highly swollen PNIPAAM has 2.8 kPa of Young's moduli at room temperature [44]. The successful mechanical failure of the microneedles was based on the cracking of PLGA microneedles caused by hydrogel expansion and the mechanical weakness of highly swollen hydrogel, as shown in Fig. 3.

3.1.2. Polymer microneedles with hydrogel particles

Responsive failure of biodegradable polymeric microneedles as a result of contact with body fluid is intended to provide sustained drug release over a predetermined period by leaving the biodegradable polymer microneedle tips and the hydrogel microparticles in the skin. The microneedles with hydrogel microparticles shown in Fig. 5(a) have a square base measuring 250 μm by 250 μm and a shaft height of 600 μm. Because the number of hydrogel microparticles encapsulated in microneedles ultimately influences the mechanical breakage of PLGA microneedles, the number of particles was controlled by varying the number of microneedles copied in the fabrication process. We quantified the number of hydrogel microparticles with a hemacytometer by counting the number of hydrogel microparticles encapsulated in the microneedles (Supplement S-1). The matrix of microneedles previously dissolved in acetonitrile, a selective solvent for PLGA. As shown in Figure S1, the hydrogel contents were increased by increasing the number of hydrogel microparticles added in cavities of microneedle mold. The average number of microparticles in an array of 100 microneedles was approximately 7000 after a single application, 12,000 after 3 applications, and 20,000 after 6 applications, corresponding to about 18%, 31%, and 53% (v/v) of average content in an array of 100 microneedles, respectively. Traditional micromolding technique was accompanied by high temperature and high pressure, resulting in the denaturation of proteins and thermally sensitive drugs. Thus, it is not easy to encapsulate thermally sensitive compounds inside a polymeric microstructure using a conventional molding process [24]. To minimize thermal damage, the polymer microparticles were used to fabricate polymer microstructures by means of ultrasonic welding [45,46]. Ultrasonic welding can be used with micromolding to fabricate polymeric microneedles with hydrogel microparticles encapsulating thermo-sensitive agents. However, the aim of the present study is restricted to exploring the feasibility of using hydrogel microparticles to cause separation of biodegradable polymer microneedles in the skin.

3.2. Insertion and failure of polymer microneedles with hydrogel particles

3.2.1. Characterization of insertion of polymer microneedles with hydrogel particles

The insertion of PLGA microneedles with hydrogel microparticles was investigated as a function of the content of hydrogel microparticles. Failure by water contact required successful insertion of microneedles into the skin. The content of hydrogel particles determined the rate of failure, and the highest possible content of hydrogel particles was recommended for quicker failure to assure successful insertion.

The successful insertion of microneedles was evaluated by applying microneedles with hydrogel microparticles on human cadaver skin. The mechanical strength of the polymer composite structure depends on the content of the composite material in the polymer matrix. Young's moduli of PLGA with 50 kDa of M.W. is about 1 GPa, and that of PNIPAAm hydrogel is reported to be about 914 kPa [47]. Thus the mechanical strength was determined by the PLGA, and the content of the PLGA is critical for successful insertion. When the insertion test was performed with microneedles with 53% (v/v) hydrogel particle content, microneedles were inserted into skin successfully as shown in Fig. 4. However, microneedles with 68% hydrogel particle content inserted only partially over the array of microneedles. Thus microneedles with 53% hydrogel particle content were appropriate for a fast response, but microneedles with 31% hydrogel particle content were used in the *in vivo* test in consideration of the marginal safety of the mechanical strength of microneedles.

3.2.2. Characterization of failure of polymer microneedles with hydrogel microparticles

To investigate the effect of volume expansion of hydrogel on mechanical failure of PLGA microneedles, microneedle failure by volume expansion was observed in terms of contact time with PBS

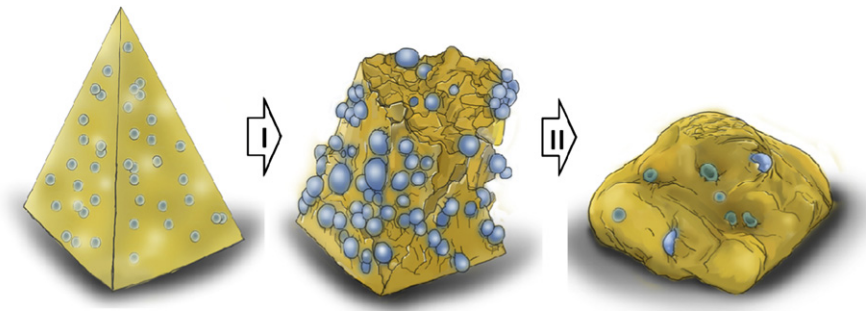

Fig. 3. Schematic diagram of mechanism of responsive failure of microneedle using volume expandable, water-absorbing hydrogel particles. (I) Hydrogel particles expand quickly by absorbing water. The quick expansion of the particles caused mechanical failure of the microneedles due to the difference in volume expansion between the needle matrix polymer and the hydrogel particles. (II) PLGA microneedles are broken by the mechanical weakness of highly swollen hydrogel and cracking of PLGA microneedles.

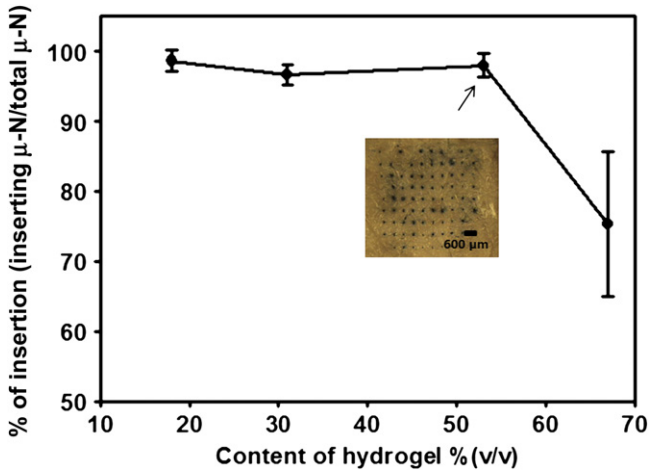

Fig. 4. The change in the ratio of the number of holes generated by microneedles to the number of microneedles concerns the content of hydrogel. Optical micrograph of the underside of human cadaver epidermis pierced by an array of polymer microneedles with (a) 18%, (b) 31%, (c) 53%, and (d) 68% (v/v) of hydrogel microparticles and subsequently exposed to Trypan Blue dye. The pattern of blue staining is the same as the array of microneedles, indicating the presence of transdermal transport pathways created in the epidermis by polymer microneedles.

without applying external force. The mechanical failure of PLGA microneedles was induced by volume expansion of hydrogel particles, as shown in Fig. 5. When PLGA microneedles encapsulating 53% (v/v) hydrogel microparticles made contact with PBS, intact microneedles were broken rapidly as a result of volume expansion of the particles. Swollen hydrogel microparticles located near the surface of the microneedle matrix broke through the surface after 10 s of contact with PBS, and microneedles began to crack after 30 s of contact. All microneedles were broken mechanically after 60 s of contact (Fig. 5(d)). This test confirmed that one failure mechanism of polymeric microneedles was induced by volume expansion of hydrogel microparticles within a PLGA microneedle matrix as a result of water absorption. Once the hydrogel microparticles began to expand on the surface of the microneedle matrix, the cracking of the microneedles quickly followed, allowing more space for water penetration and leading to rapid breakdown of the matrix. Water should penetrate the PLGA microneedle matrix to make contact with the hydrogel microparticles and delayed contact retards volume expansion of the particles.

A needle failure test also was performed by inserting microneedles into the full thickness of porcine cadaver skin *in vitro* to determine how long microneedle tips should be inserted in the porcine cadaver skin for successful separation of microneedle tips. External force was applied to insert the microneedles into the porcine cadaver skin, and water contact and external force were considered factors for needle failure. As shown in Fig. 6, swelling of hydrogel microparticles in porcine cadaver skin was insignificant at 60 s, whereas 60 s of contact with PBS was sufficient to induce failure of the microneedles (Fig. 5(d)). Most microneedle tips broke down in porcine cadaver skin after 15 min of insertion. Water content in skin ranges from 20% to 60% depending on the layer of skin [48], and the response of hydrogel particles to water in porcine cadaver skin is slower than to PBS. Needle failure began from the end of the microneedle tips, as shown in Fig. 6. This is because water content increased gradually from the upper part of the stratum corneum down to the epidermis, resulting in more water absorption near the tip apex. Hydrogel microparticles were found near the surface of the microneedles initially, but only a few intact microparticles were found after 30 min of insertion into the skin.

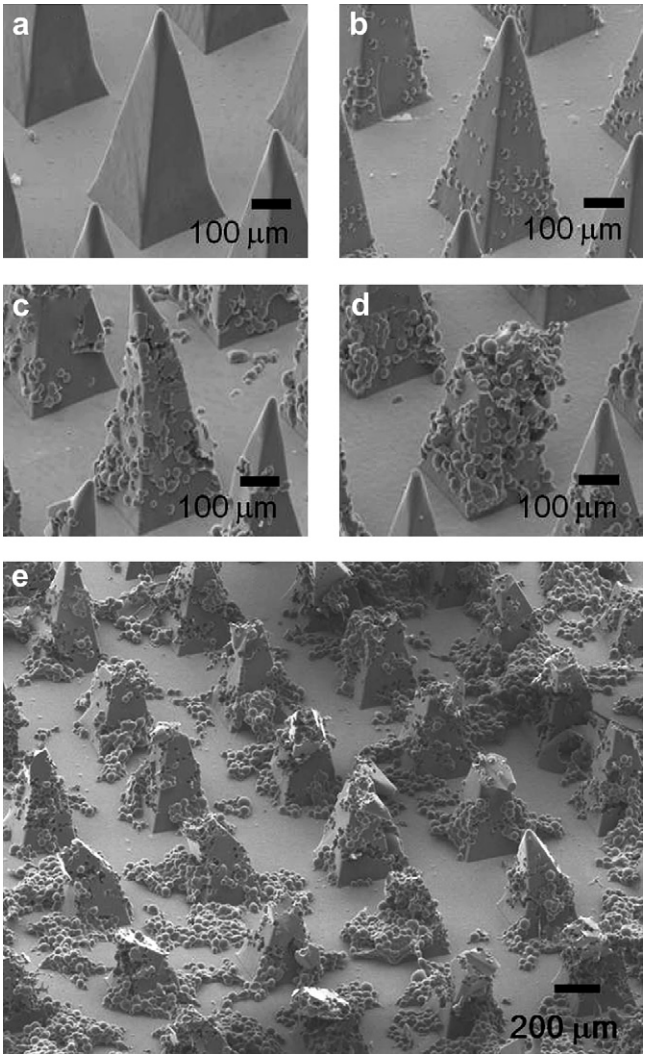

Fig. 5. SEM image of morphological change in microneedles with hydrogel microparticles regarding contact duration with PBS (a) 0 s, (b) 10 s, (c) 30 s, and (d) 60 s. SEM image of all microneedles broken mechanically after 60 s of contact (e). Microneedles were made of PLGA and 53% (v/v) of hydrogel particles were encapsulated in an array of microneedles.

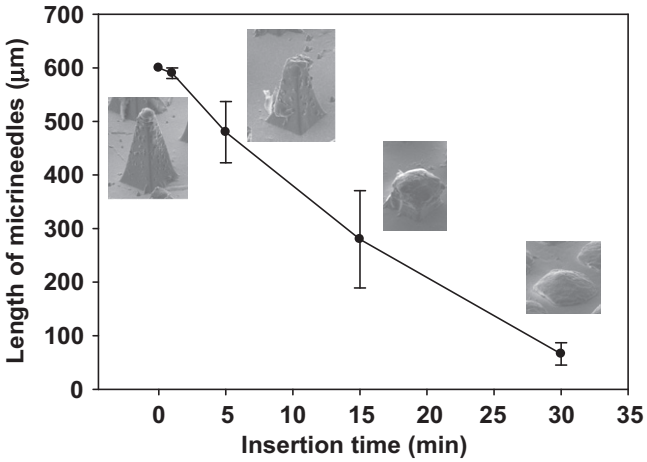

Fig. 6. SEM images of morphological change in PLGA microneedles with hydrogel microparticles inserted into porcine cadaver skin for 1 min, 5 min, 15 min, and 30 min with constant 20 N of compression force. Microneedles were made of PLGA and 31% (v/v) of hydrogel particles were encapsulated in an array of microneedles.

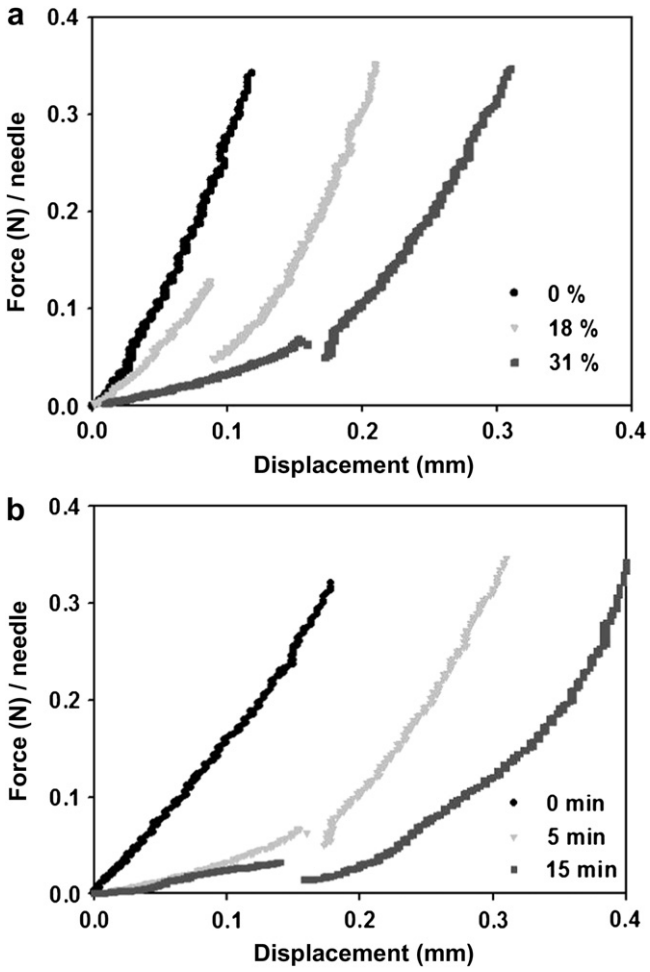

Fig. 7. Mechanical behavior of PLGA microneedles. Force measured as a microneedle displacement while pressing against a rigid surface (a) PLGA microneedles having 0%, 18%, and 31% (v/v) of hydrogel particles after 5 min exposure to PBS (b) PLGA microneedles with 31% (v/v) of hydrogel particles after exposure to PBS for 0 min, 5 min, and 15 min.

This result confirms that the swelling of hydrogel microparticles initiates the cracking of PLGA microneedles and then the hydrogel is crushed by external force caused by insertion and removal due to the low mechanical strength of highly swollen hydrogel microparticles.

To obtain more comprehensive data, polymer needles are pressed at constant velocity into a hard metal surface while needle force and displacement are continuously measured. The mechanical behavior of microneedles is shown in Fig. 7. The force-displacement curve (which is analogous to a stress–strain curve) exhibited a nonlinear differential modulus, which is parameterized in terms of content of hydrogel microparticles and exposure time to water. Comparison of the slope of the stress–strain curve, as presented in Fig. 7, shows that the steeper the stress–strain relationship, the stiffer the material. After 5 min of contact with PBS, solid PLGA microneedles are stiff and PLGA microneedles with 31% (v/v) hydrogel microparticle content are more ductile. There was a minor change in the slope of solid PLGA microneedles after water exposure (data not shown here). PLGA microneedles with 18% (v/v) hydrogel microparticle content deformed less than those with 31% and more than solid PLGA, as shown in Fig. 7(a). For 100 μm of displacement, PLGA microneedles with 31% (v/v) hydrogel microparticle content have less than one tenth the force of solid PLGA microneedles. As expected, the increase in hydrogel content significantly decreased the mechanical strength of the microneedles after water contact. Microneedle disruption is indicated by the drop in applied force, and this may have happened at the interface of swollen hydrogel particles and PLGA. After 15 min of contact time with water, PLGA microneedles with 31% (v/v) hydrogel microparticle content have less than one-twentieth the force of non-exposed PLGA microneedles with the same hydrogel microparticle content for 200 μm of displacement, as shown in Fig. 7(b). This result confirms that more exposure to water induced more swelling of hydrogel microparticles, resulting in easy deformation and disruption of PLGA microneedles because of mechanical weakness of hydrogel and cracking of PLGA microneedles.

To compare the failure mechanism, PLGA microneedles containing hydrogel particles were compared with solid PLGA microneedles and PLGA microneedles containing salt particles. After all microneedles were inserted into the back of a hairless mouse for 1 h *in vivo*, microneedles with hydrogel particles showed breakdown, whereas solid PLGA microneedles were intact (Fig. 8(a)). PLGA microneedles with salt particles had pores of 1–4 μm in diameter on the surface and almost intact bent tips were obtained after removal, as shown in Fig. 8(b). The comparison with solid PLGA microneedles showed that separation of PLGA microneedles was successful as a result of the swelling of the hydrogel microparticles. Also, the comparison with microneedles with salt particles demonstrated that volume expansion of hydrogel particles accelerated the generation of a water pathway, resulting in rapid mechanical failure of the microneedles. Contact with water at the surface of microneedles with hydrogel microparticles and with salt particles extended for the same duration. However, volume expansion of hydrogel particles produced a quicker breakdown, reducing the insertion time of the microneedle tips and thus improving patient convenience.

3.2.3. *Stability of microneedles with hydrogel particles in high humidity*

Microneedles with hydrogel microparticles were responsive to water contact. Thus the response to high humidity was observed because the storage stability of microneedles with hydrogel particles can be a critical issue in fully developing this new system. By comparing water-dissolving microneedles, resistance to high humidity was evaluated. Up to 1 h, there was no difference in

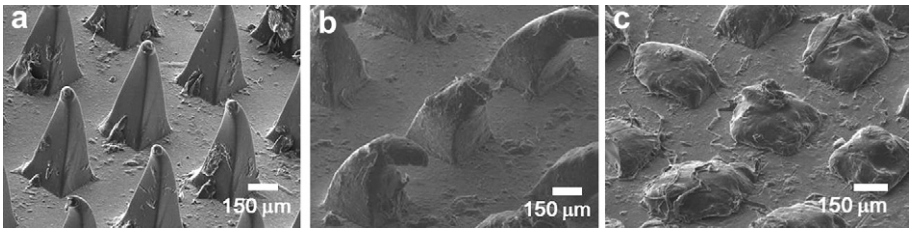

Fig. 8. SEM images of morphological changes in (a) poly-lactic-co-glycolic (PLGA) microneedles (b) salt particle integrated microneedles (about 30% (v/v)) (c) hydrogel particle integrated microneedles (31% (v/v)) after insertion into the back skin of a hairless mouse for 1 h.

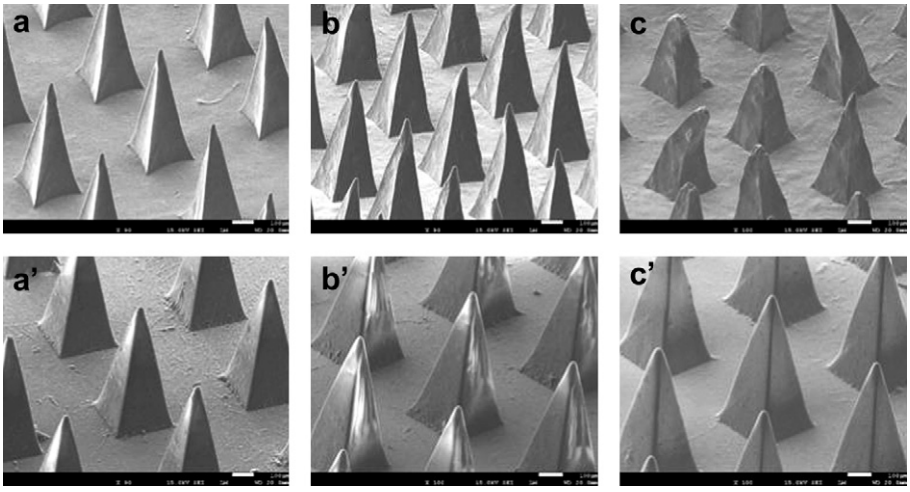

Fig. 9. SEM images of morphological change in (a, b, c) water-soluble microneedles made of carboxy-methyl-cellulose and (a′, b′, c′) hydrogel particle integrated microneedles (31% (v/v)) in high humidity (95%) at 1 h (a, a′), 5 h (b, b′), and 12 h (c, c′).

morphological changes between water-dissolving microneedles made of carboxymethyl cellulose (CMC) and microneedles with hydrogel microparticles. The tips of CMC microneedles turned blunt by absorbing water at 5 h, but PLGA microneedles with hydrogel particles remained in their initial shape. The morphological change resulting from high humidity was more significant at 12 h, as shown in Fig. 9(c). While hydrogel microparticles absorbed water rapidly, a thin PLGA film on the microneedles served as a protective layer

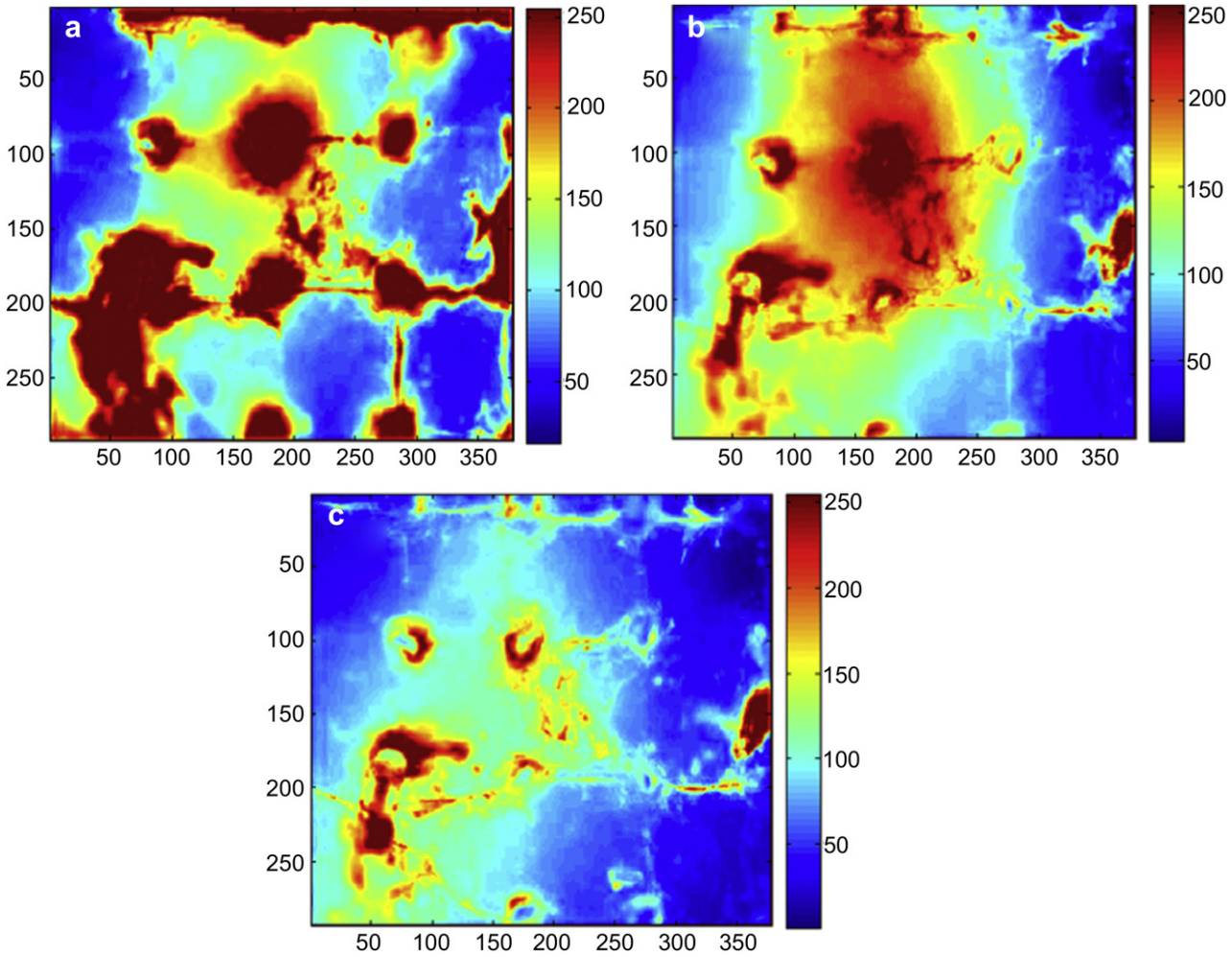

Fig. 10. Time-lapsed images showing the decrease in fluorescent intensity in porcine cadaver skin due to the diffusion of calcein through the skin. Fluorescence microscopy images of calcein delivered into porcine cadaver skin using polymer microneedles are shown. A 100-needle array of PLGA microneedles containing hydrogel particles with calcein was inserted into full thickness cadaver skin for 15 min. The skin was imaged by fluorescence microscopy at (a) 0, (b) 15, and (c) 60 min after removal of the needles.

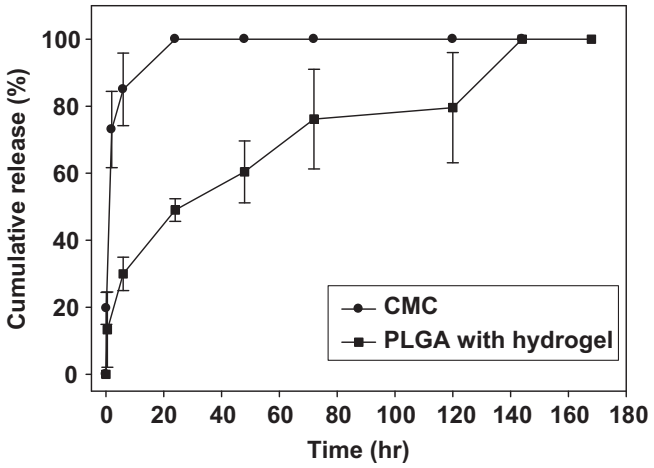

Fig. 11. Release profile of PLGA microneedles containing hydrogel and rhodamine and CMC microneedles with rhodamine as function of time.

against humidity. The amount of water absorbed in hydrogel microparticles was retarded by the thin PLGA layer. However, direct contact with water weakened the resistance of the PLGA layer to water as a result of swelling of PLGA by water uptake [49].

3.3. Drug delivery property of microneedles with hydrogel microparticles

3.3.1. Drug delivery property of hydrogel particles

In order to evaluate the feasibility of hydrogel as a carrier of hydrophilic drugs, microneedles with hydrogel microparticles were pre-incubated in a calcein solution. The hydrophilic model drug can be tracked over time by the green fluorescence of calcein, which was diffused through porcine cadaver skin surface (Fig. 10). Calcein diffused out in all directions through the skin around penetration sites over time. The initial intensity of calcein immediately after insertion was strong near insertion points for 15 min, but the intensity weakened over time. This evaluation suggests that a hydrophilic model drug can be delivered by hydrogel particles, and the release rate can be manipulated by controlling the properties of the hydrogel particles. We confirmed that hydrogel microparticles were delivered successfully into the skin by hydrogel swelling and that hydrogel was very quickly exposed to the skin layer once the microneedles were inserted. Fast exposure of hydrogel to the skin layer facilitated quick delivery of calcein into the skin layer. As shown in Fig. 10, the intensity of calcein around penetration sites became much weaker after 1 h, showing that most of the calcein was diffused out over the skin layer. Various types of hydrogel particles have been developed to control the drug release rate, and controlled delivery of a hydrophilic model drug will be possible by utilizing the physical and chemical properties of various types of pre-developed hydrogel.

3.3.2. Drug delivery property of biodegradable polymeric microneedles in vitro

A drug release test was performed by inserting CMC microneedles and PLGA microneedles with hydrogel into epidermis for 1 h. After 1 h, both PLGA and CMC microneedle arrays remained in the epidermis, enabling them to serve as a drug depot. Fig. 11 shows that 85% of the rhodamine was released from the CMC microneedles within 6 h of being placed in a PBS receptor compartment, indicating that CMC microneedles had fast release and that their release pattern depended on dissolution of CMC and rhodamine salt. Fast release of all rhodamine into the receptor was expected because of the quick dissolution of CMC in water. However, some portion of CMC microneedles with rhodamine was placed above the stratum corneum, slowing dissolution of the bottom part of the microneedles in the receptor and resulting in 100% release after 6 h. For the PLGA microneedles, 60% of the rhodamine was released after approximately 2 days in PBS, suggesting that their release pattern depended on bulk diffusion of rhodamine rather than the slower polymer degradation because rhodamine salt particles were distributed in a PLGA microneedle array and the degradation time of PLGA is 1–2 months. However, if a model drug is distributed through PLGA microneedles at the molecular level, the release profile that depends on PLGA degradation can be obtained. PLGA microneedles with hydrogel microparticles can deliver the needle array into the skin by insertion in less than 1 h, and the remaining needle array in the skin can release the drug over a few days to a few months by diffusion of drug and degradation of the PLGA microneedle array. A patch application also can be used for

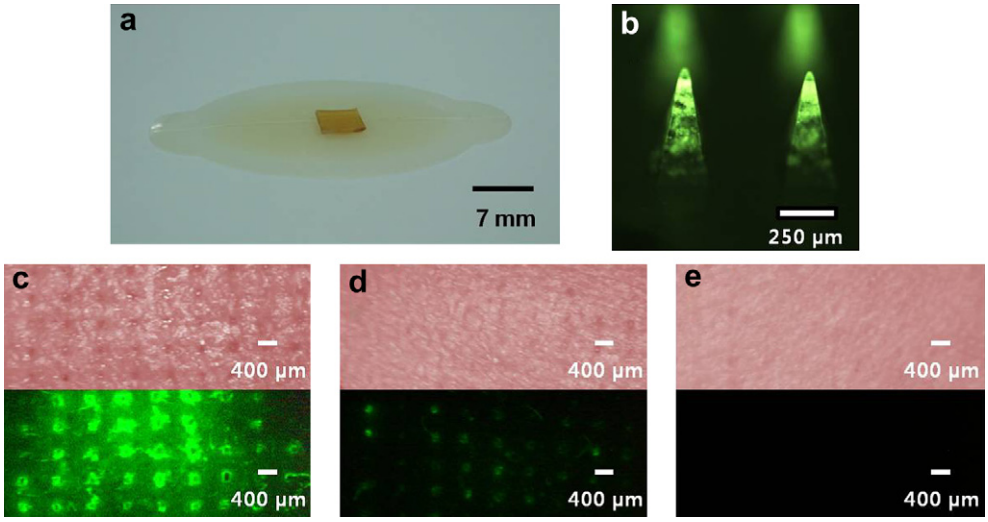

Fig. 12. (a) Microneedle system attached on the bandage. (b) Fluorescent microscopic image of microneedles with fluorescence-tagged hydrogel microparticles (c–e). Optical light microscopic image (top) and fluorescent microscopic image (bottom) of hairless mouse skin *in vivo* at (c) 1 h, (d) 1 day, and (e) 3 days after insertion of microneedles with fluorescence-tagged hydrogel microparticles for 30 min. An array of PLGA 50/50 microneedles with hydrogel particles in 100 microneedles (31% (v/v)) was inserted into mouse skin *in vivo*.

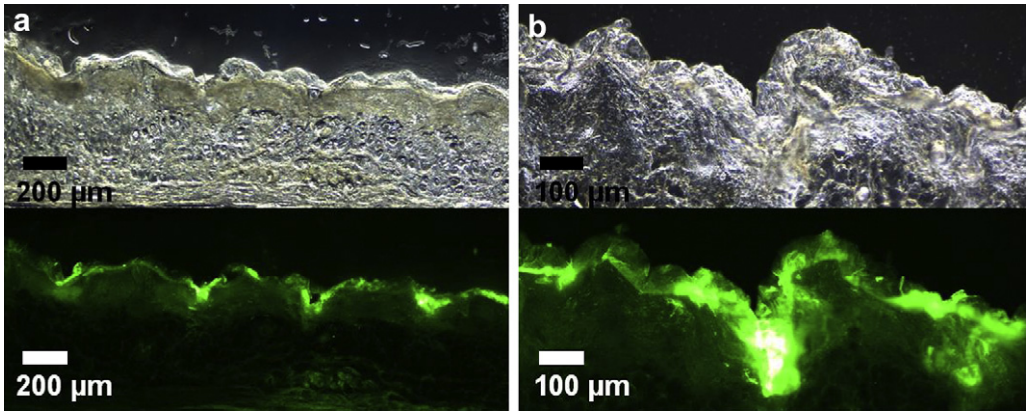

Fig. 13. Transdermal drug delivery test using *in vivo* mouse. PLGA microneedles containing fluorescence-tagged hydrogel particles in the rat skin after needle insertion for 60 min are shown. Vertical skin sections of penetration sites were investigated by optical microscopy (top) and fluorescence microscope (bottom) increasing magnification from (a) to (b).

sustained release of a drug after the skin is pierced using solid microneedles, but the patch should remain adhered to the skin for a longer period over a few days to deliver the drug through holes in the skin [15]. Another concern of drug delivery through holes in the skin is that the holes close in a few hours, resulting in the reduction of the delivery rate. This new system of transdermal drug delivery through microneedles can achieve safe, sustained drug release for a predetermined period because the remaining PLGA microneedle array degrades by hydrolysis within a few months.

3.3.3. *Drug delivery property of biodegradable polymeric microneedles in vivo*

Tips of microneedles remaining in skin were investigated using fluorescence-tagged hydrogel microparticles in the microneedles (Fig. 12). To examine whether the LCST change occurred by copolymerization of PNIPAAm gels with AAc through fluorescent FITC labeling, LCST of modified and primitive PNIPAAm hydrogels was investigated by difference scanning calorimeter (DSC). DSC thermogram showed that LCST value of P(NIPAAm-*co*-AA) hydrogels (32.8 °C) was almost similar to that of unmodified PNIPAAm hydrogels (31.4 °C), indicating that the chemical modification of PNIPAAm did not significantly affect thermal behavior of P(NIPAAm-*co*-AA) hydrogels (Figure S2). Fluorescence was tagged on the surface of hydrogel particles and the change of microneedles in *in vivo* skin was scanned for 3 days. Microneedles were applied using a hydrogel bandage for a predetermined term (Fig. 12(a)). The application by bandage provided good contact between microneedles and skin, ease of use, and prevention of dry skin [48]. Fluorescence-tagged hydrogel microparticles were located in microneedles and the intensity of fluorescence was maintained after the PLGA molding process, as shown in Fig. 12(b).

Microneedle tips were found in the skin immediately after insertion of microneedles with fluorescence-tagged hydrogel microparticles for 30 min, as shown in Fig. 12(c). Their exposure was confirmed by SEM observation (Figure S3). Sites of solid microneedle penetration have been studied by staining with Trypan Blue [9] because it was difficult to find the penetration sites by optical microscope due to the tiny size of the holes [50]. Compared to insertion sites caused by solid microneedle penetration using a microneedle roller, insertion sites caused by microneedles with hydrogel microparticles were easily seen with an optical microscope at 10× of magnification, as shown in Fig. 12(c), because the tips remain. As shown in Fig. 12(d) and (e), the insertion sites were still visible after 1 day, and the ends of the tips were covered with skin after 3 days. Skin recovery over tips of PLGA microneedles with hydrogel microparticles was slower than that over holes generated by other microneedle methods such as a solid microneedle or a dissolving microneedle. Penetration sites were difficult to found even immediately after insertion and removal of solid microneedles [50] and a few hours after insertion and removal of water-dissolving microneedles. Skin recovery rate is an important factor for determining drug delivery method and safety. Even though holes are blocked by microneedle tips, very tiny crevices around microneedles may exist [50]. Thus drug may be delivered through the crevices around microneedles [7]; however, it may be difficult for microbes to penetrate through the crevices because the crevices are extremely small [51]. By integrating microneedles into the patch system, PLGA microneedle tips embedded in skin can serve as the transport pathway through the skin over a few days. After 3 days, the ends of microneedle tips were difficult to find using an optical microscope, and the intensity of fluorescence was not found with a fluorescence microscope either. The loss of fluorescence intensity can be attributed to skin recovery. After 3 days *in vitro*, tagged fluorescence intensity on hydrogel microparticles in PBS remained. Thus it can be concluded that skin recovery over microneedles tips induced the loss of fluorescence intensity.

PLGA microneedles containing hydrogel microparticles were investigated after being inserted in mouse skin for 60 min. As shown in Fig. 13, penetration sites were investigated by optical microscopy (top of Fig. 13) and fluorescence microscope (bottom of Fig. 13); magnification was also increased (Fig. 13(a) and (b)). Hydrogel microparticles were placed over the stratum corneum, epidermis and the dermis layers, and they stayed near penetration sites. The implantation of tips of biodegradable polymeric microneedles with hydrogel particles can achieve local delivery of depot drugs through the skin, and long-term delivery of drugs is possible by utilizing the sustained release property of biodegradable polymer and hydrogel microparticles.

4. Conclusions

The tips of biodegradable polymeric microneedles encapsulating volume expandable, water-absorbing hydrogel microparticles were separated after being inserted into the skin because hydrogel microparticles expand quickly and highly swollen hydrogel loses mechanical strength rapidly. This method utilizes the difference in volume expansion between the needle matrix polymer (PLGA) and the encapsulated hydrogel microparticles and low mechanical strength of highly swollen hydrogel. The content of hydrogel particles defined the rate of microneedle failure. Microneedle tips with hydrogel microparticles were successfully left behind in porcine cadaver skin *in vitro* and in hairless mouse skin *in vivo* within less than 1 h of insertion into skin by swelling of hydrogel microparticles. Fast delivery and sustained delivery of

drug could be achieved by utilizing the drug delivery property of hydrogel and biodegradable polymer. Remaining PLGA tips with rhodamine salt could release drugs over a few days below the epidermis. This new system can provide practical and efficient transdermal drug delivery by leaving biodegradable polymeric microneedles in skin and by offering easy fabrication, patient convenience, and responsive interaction. This new microneedle system can be improved by combining it with pre-developed hydrogel techniques for providing versatile sustained release methods.

Acknowledgments

We thank Yong-Youn Hwang and Gi-An Um at SK Chemicals for helpful discussion and Min-Ji Kim for drawing a figure of the failure mechanism. We also thank friends at the Georgia Institute of Technology for help in measurement of stress–strain behavior and Dr. Jong-Chul Jung for color-mapping of the fluorecence image. This work was supported by the GRRC program of Gyeonggi province [GRRC Kyungwon 2011-B04, Development of Microfluidic Chip for diagnosis of disease].

Appendix. Supplementary material

Supplementary material associated with this article can be found, in the online version, at doi:10.1016/j.biomaterials.2011.09.074.

References

[1] Kost J. Smart polymers for controlled release. In: Wise DL, editor. Handbook of pharmaceutical controlled release technology. New York: Marcel Dekker Inc; 2000. p. 65–88.
[2] Hatefi A, Amsden B. Biodegradable injectable in situ forming drug delivery systems. J Control Release 2002;80:9–28.
[3] Samad A, Sultana Y, Aqil M. Liposomal drug delivery systems: an update review. Curr Drug Deliv 2007;4:297–305.
[4] Prausnitz MR, Langer R. Transdermal drug delivery. Nat Biotechnol 2008;26:1261.
[5] Naik A, Kalia YN, Guy RH. Transdermal drug delivery: overcoming the skin's barrier function. Pharm Sci Technol Today 2000;3:318–26.
[6] Li G, Badkar A, Nema S, Kolli CS, Banga AK. *In vitro* transdermal delivery of therapeutic antibodies using maltose microneedles. Int J Pharm 2009;368:109–15.
[7] Martanto W, Davis SP, Holiday N, Wang J, Gill H, Prausnitz MR. Transdermal delivery of insulin using microneedles *in vivo*. Pharm Res 2004;21:947–52.
[8] Ding Z, Verbaan FJ, Bivas-Benita M, Bungener L, Huckriede A, van den Berg DJ, et al. Microneedle arrays for the transcutaneous immunization of diphtheria and influenza in BALB/c mice. J Control Release 2009;136:71–8.
[9] McAllister DV, Wang PM, Davis SP, Park JH, Canatella PJ, Allen MG, et al. Microfabricated needles for transdermal delivery of macromolecules and nanoparticles: fabrication methods and transport studies. Proc Natl Acad Sci U S A 2003;100:13755–60.
[10] Coulman SA, Anstey A, Gateley C, Morrissey A, McLoughlin P, Allender C, et al. Microneedle mediated delivery of nanoparticles into human skin. Int J Pharm 2009;366:190–200.
[11] Banks SL, Pinninti RR, Gill HS, Paudel KS, Crooks PA, Brogden NK, et al. Transdermal delivery of naltrexol and skin permeability lifetime after microneedle treatment in hairless guinea pigs. J Pharm Sci 2010;99:3072–80.
[12] Lee JW, Park J-H, Prausnitz MR. Dissolving microneedles for transdermal drug delivery. Biomaterials 2008;29:2113–24.
[13] Sullivan SP, Koutsonanos DG, del Pilar Martin M, Lee JW, Zarnitsyn V, Choi SO, et al. Dissolving polymer microneedle patches for influenza vaccination. Nat Med 2010;16:915–20.
[14] Prausnitz MR. Microneedles for transdermal drug delivery. Adv Drug Deliv Rev 2004;56:581–7.
[15] Park J-H, Choi S-O, Seo S, Choy YB, Prausnitz MR. A microneedle roller for transdermal drug delivery. Eur J Pharm Biopharm 2010;76:282–9.
[16] Gill HS, Prausnitz MR. Coated microneedles for transdermal delivery. J Control Release 2007;117:227–37.
[17] Cormier M, Johnson B, Ameri M, Nyam K, Libiran L, Zhang DD, et al. Transdermal delivery of desmopressin using a coated microneedle array patch system. J Control Rel 2004;97:503–11.
[18] Koutsonanos DG, del Pilar Martin M, Zarnitsyn VG, Sullivan SP, Compans RW, Prausnitz MR, et al. Transdermal influenza immunization with vaccine-coated microneedle arrays. PLoS One 2009;4:4773.
[19] Sullivan SP, Murthy N, Prausnitz MR. Minimally invasive protein delivery with rapidly dissolving polymer microneedles. Adv Mater 2008;20:933–8.
[20] Erdos G, Donahue C, Williams M, Ozdoganlar B, Falo L. Biodegradable dissolving microneedle arrays effectively deliver antigens and adjuvants to skin DCs for the induction of antigen specific immune responses. J Immunol 2010;184. 48.12.
[21] Chu LY, Choi SO, Prausnitz MR. Fabrication of dissolving polymer microneedles for controlled drug encapsulation and delivery: bubble and pedestal microneedle designs. J Pharm Sci 2010;99:4228–38.
[22] Ito Y, Yoshimitsu JI, Shiroyama K, Sugioka N, Takada K. Self-dissolving microneedles for the percutaneous absorption of EPO in mice. J Drug Target 2006;14:255–61.
[23] Fukushima K, Ise A, Morita H, Hasegawa R, Ito Y, Sugioka N, et al. Two-layered dissolving microneedles for percutaneous delivery of peptide/protein drugs in rats. Pharm Res 2011;28:1–15.
[24] Park JH, Allen MG, Prausnitz MR. Polymer microneedles for controlled-release drug delivery. Pharm Res 2006;23:1008–19.
[25] Zhang H, Zhong H, Zhang L, Chen S, Zhao Y, Zhu YL, et al. Modulate the phase transition temperature of hydrogels with both thermosensitivity and biodegradability. Carbohydr Polym 2010;79:131–6.
[26] Yoshida R, Okano T. Stimuli-responsive hydrogels and their application to functional materials. In: Park K, Okano T, editors. Biomedical applications of hydrogels handbook. New York: Springer; 2010. p. 19–43.
[27] Lin CC, Metters AT. Hydrogels in controlled release formulations: network design and mathematical modeling. Adv Drug Deliv Rev 2006;58:1379–408.
[28] Nguyen KT, West JL. Photopolymerizable hydrogels for tissue engineering applications. Biomaterials 2002;23:4307–14.
[29] Kissel T, Li Y, Unger F. ABA-triblock copolymers from biodegradable polyester A-blocks and hydrophilic poly (ethylene oxide) B-blocks as a candidate for in situ forming hydrogel delivery systems for proteins. Adv Drug Deliv Rev 2002;54:99–134.
[30] Qiu Y, Park K. Environment-sensitive hydrogels for drug delivery. Adv Drug Deliv Rev 2001;53:321–39.
[31] Ruel-Gariepy E, Leroux JC. In situ-forming hydrogels–review of temperature-sensitive systems. Eur J Pharm Biopharm 2004;58:409–26.
[32] Kozlovskaya V, Kharlampieva E, Mansfield ML, Sukhishvili SA. Poly (methacrylic acid) hydrogel films and capsules: response to pH and ionic strength, and encapsulation of macromolecules. Chem Mater 2006;18:328–36.
[33] Hennink W, Van Nostrum C. Novel crosslinking methods to design hydrogels. Adv Drug Deliv Rev 2002;54:13–36.
[34] Hoffman AS. Hydrogels for biomedical applications. Adv Drug Deliv Rev 2002;54:3–12.
[35] Kim SW, Bae YH, Okano T. Hydrogels: swelling, drug loading, and release. Pharm Res 1992;9:283–90.
[36] Zhao C, Zhuang X, He P, Xiao C, He C, Sun J, et al. Synthesis of biodegradable thermo-and pH-responsive hydrogels for controlled drug release. Polymer 2009;50:4308–16.
[37] Zhang Z, Chen L, Zhao C, Bai Y, Deng M, Shan H, et al. Thermo-and pH-responsive HPC-g-AA/AA hydrogels for controlled drug delivery applications. Polymer 2010;52:676–82.
[38] Takezawa T, Mori Y, Yoshizato K. Cell culture on a thermo-responsive polymer surface. Nat Biotechnol 1990;8:854–6.
[39] von Buelow S, Pallua N. Efficacy and safety of polyacrylamide hydrogel for facial soft-tissue augmentation in a 2-year follow-up: a prospective multicenter study for evaluation of safety and aesthetic results in 101 patients. Plast Reconstr Surg 2006;118:85S–91S.
[40] Kim S, Healy KE. Synthesis and characterization of injectable poly (N-isopropylacrylamide-co-acrylic acid) hydrogels with proteolytically degradable cross-links. Biomacromolecules 2003;4:1214–23.
[41] Bertrand N, Fleischer JG, Wasan KM, Leroux JC. Pharmacokinetics and biodistribution of N-isopropylacrylamide copolymers for the design of pH-sensitive liposomes. Biomaterials 2009;30:2598–605.
[42] Gao D, Xu H, Philbert MA, Kopelman R. Bioeliminable nanohydrogels for drug delivery. Nano Lett 2008;8:3320–4.
[43] Ohlson M, Sörensson J, Haraldsson B. Glomerular size and charge selectivity in the rat as revealed by FITC-Ficoll and albumin. Am J Physiol Renal Physiol 2000;279:F84–91.
[44] Matzelle T, Ivanov D, Landwehr D, Heinrich L, Herkt-Bruns C, Reichelt R, et al. Micromechanical properties of "smart" gels: studies by scanning force and scanning electron microscopy of PNIPAAm. J Phys Chem B 2002;106:2861–6.
[45] Park JH, Choi SO, Kamath R, Yoon YK, Allen MG, Prausnitz MR. Polymer particle-based micromolding to fabricate novel microstructures. Biomed Microdevices 2007;9:223–34.
[46] Min J, Park JH, Yoon HH, Choy YB. Ultrasonic welding method to fabricate polymer microstructure encapsulating protein with minimum damage. Macromol Res 2008;16:570–3.
[47] Muniz E, Geuskens G. Polyacrylamide hydrogels and semi-interpenetrating networks (IPNs) with poly (N-isopropylacrylamide): mechanical properties by measure of compressive elastic modulus. J Mater Sci Mater Med 2001;12:879–81.
[48] Caspers PJ, Lucassen GW, Carter EA, Bruining HA, Puppels GJ. *In vivo* confocal Raman microspectroscopy of the skin: noninvasive determination of molecular concentration profiles. J Invest Dermatol 2001;116:434–42.
[49] Sharp J, Forrest J, Jones R. Swelling of poly (DL-lactide) and polylactide-co-glycolide in humid environments. Macromolecules 2001;34:8752–60.
[50] McAllister DV. Microfabricated needles for transdermal drug delivery. doctoral dissertation. Atlanta: Georgia Institute of Technology; 2000.
[51] McAllister DV, Allen MG, Prausnitz MR. Microfabricated microneedles for gene and drug delivery. Annu Rev Biomed Eng 2000;2:289–313.